Atmos. Chem. Phys. Discuss., https://doi.org/10.5194/acp-2018-1072
Manuscript under review for journal Atmos. Chem. Phys.
Discussion started: 16 November 2018


Atmospheric Chemistry and Physics
Open Access
Discussions

# Diurnal variation of heavy rainfall over the Beijing-Tianjin-Hebei region: Role of aerosol cloud effect and its sensitivity to moisture

Siyuan Zhou[1], Jing Yang[1,2*], Chuanfeng Zhao[2,3], Wei-Chyung Wang[4], Daoyi Gong[1,2], Peijun Shi[1,2]

[1] Academy of Disaster Reduction and Emergency Management, Faculty of Geographical Science, Beijing Normal University, China
[2] State Key Laboratory of Earth Surface Process and Resource Ecology, Beijing Normal University, China
[3] College of Global Change and Earth System Science, Beijing Normal University, China
[4]Atmospheric Sciences Research Center, State University of New York, Albany, New York 12203, USA

Submitted to ACP
Oct 2018

*Correspondence to: Jing Yang, State Key Laboratory of Earth Surface Process and Resource Ecology/Academy of Disaster Reduction and Emergency Management, Faculty of Geographical Science, Beijing Normal University, 19#Xinjiekouwai Street, Haidian District, Beijing 100875, China. E-mail: yangjing@bnu.edu.cn

Atmos. Chem. Phys. Discuss., https://doi.org/10.5194/acp-2018-1072
Manuscript under review for journal Atmos. Chem. Phys.
Discussion started: 16 November 2018


**Abstract:** Our recent study found that, during 2002-2012, the diurnal variation of heavy rainfall over Beijing-Tianjin-Hebei (BTH) region exhibits different characteristics between clean and polluted environment. Here we use satellite cloud–products together with meteorology and aerosol data to further examine the aerosol impact on the associated clouds focusing on its sensitivity to moisture. During the days with large aerosol loading, the characteristics of earlier starting time, earlier peak hour and the longer duration of heavy rainfall are usually accompanied by increased cloud fraction, reduced cloud top height and increased/reduced liquid/ice effective radius. However, the aerosol effects on the cloud top and liquid effective radius are distinct at lower and higher humidity. Different from the radiative effect that black carbon heats the lower troposphere and may generate the earlier start of heavy rainfall, the aerosol cloud effect enhances the efficiency of precipitation and advances the rainfall peak, which may be ascribed to increased cloud droplet number and cloud water, enhanced collision-coalescence and accelerated rainfall formation when the background moisture supply is sufficient. The speculation warrants further numerical experiment to verify.

**Key words: aerosol, heavy rainfall, diurnal variation, cloud, Beijing-Tianjin-Hebei, observational study**

## 1. Introduction

Aerosols modify the global hydrologic cycle through both radiative effect (direct effect) and cloud effect (indirect effect) (IPCC, 2013). On the one hand, through absorbing or scattering solar radiation, aerosols can lead to the air aloft heating (e.g. Jacobson 2001; Lau et al. 2006) or the surface cooling (Lelieveld and Heintzenberg 1992; Guo et al. 2013; Yang et al., 2018), which changes the atmospheric vertical static stability and modulates rainfall (e.g. Rosenfeld et al. 2008). On the other hand, water-soluble aerosols serving as cloud condensation nuclei (CCN) could affect the warm-rain processes and cold-rain processes through influencing the cloud droplet size distributions, cloud top heights and the depth of the mixed-phase cloud (Jiang et al., 2002; Givati and Rosenfeld 2004; Chen et al., 2011; Lim and Hong 2012; Tao et al., 2012). Beijing-Tianjin-Hebei (BTH) region is the heaviest aerosol polluted area in China and concerns have been raised about the aerosol-radiation-cloud-precipitation interaction over this region. The impact of aerosols on light rainfall or warm-rain processes over BTH region almost reaches consistent agreement (e.g., Qian et al., 2009), but aerosols impact on the heavy convective rainfall in this region still has large uncertainties (Wang et al., 2009; Guo et al., 2014; Wang et al., 2016).

The clouds that can generate the heavy convective rainfall in BTH region usually contain warm clouds, cold clouds and mixed-phase clouds (e.g. Guo et al., 2015). Due to the complicacy of these clouds, aerosol indirect effect on associated clouds of heavy rainfall is more complicated than its direct effect (Sassen et al., 1995; Sherwood, 2002; Jiang et al., 2008, Tao et al., 2012). For warm clouds, by serving as CCN for more cloud droplets, aerosols can increase cloud albedo (Twomey, 1977), increase the cloud lifetime (Albrecht, 1989), and enhance thin cloud thermal emissivity (Garrett and Zhao, 2006), which were collectively known as

Twomey effect. Twomey effect increases cloud microphysical stability and suppresses warm-rain processes (Albrecht 1989; Rosenfeld et al. 2014). For cold clouds and mixed-phase clouds, many studies reported that the cloud liquid accumulated by aerosols is converted to ice hydrometeors above the freezing level, which invigorates deep convective clouds and intensifies heavy precipitation so called invigoration effect (Rosenfeld and Woodley, 2000; Rosenfeld et al., 2008; Lee et al. 2009; Guo et al. 2014). However, due to the different condition of moisture, the contrary results of aerosol impact on clouds have been also reported in observations. e.g., “Anti-Twomey” effect denotes that the cloud droplet effective radius increases with aerosol amount when the environment has a plenty of moisture supply (Yuan et al., 2008; Bulgin et al., 2008; Panicker et al., 2010; Jung et al., 2013; Harikishan et al., 2016; Qiu et al., 2017). Besides, the influence of aerosols on ice clouds also depends upon the moisture content (Jiang et al., 2008). Therefore, how the aerosols modify the clouds associated with heavy convective rainfall does not reach a consensus, particularly if considering different moisture conditions.

Heavy convective rainfall usually occurs within one day. Several previous studies have found that the aerosols can modify the rainfall diurnal variation in other regions of China (Fan et al., 2015; Guo et al., 2016; Lee et al., 2016). However, the above studies do not address the changes of associated cloud features and don’t include the different moisture conditions. Although our recent work over BTH region (Zhou et al. 2018) attempted to remove the meteorological effect including moisture and circulation and found that the peak of heavy rainfall diurnal variations shifts earlier under polluted condition, it only excluded the extreme moisture conditions and focused on aerosol radiative effect on the rainfall diurnal variation. Therefore, this study aims to deepen the previous study (Zhou et al., 2018) and extends the investigation into the following questions: (1) how do aerosols modify different features of diurnal rainfall variation (starting time, peak time and duration)? (2) how do aerosols influence cloud characteristics with inclusion of moisture condition? (3) what distinct roles do the aerosol radiative effect and cloud effect play on the different developing phase of heavy rainfall in diurnal variation? To solve the questions, the paper is organized as following: The data and methodology are introduced in Sect. 2. Section 3 presents the distinct characteristics of rainfall diurnal variation on clean/polluted days. Section 4 addresses the aerosol effect on cloud with inclusion of moisture. Section 5 discusses the distinct roles of the radiative effect and cloud effect of aerosols that play on diurnal variation of heavy rainfall. Conclusion will be given in Sect. 6.

## 2. Data and methodology

### 2.1 Data

Four types of datasets from the year 2002 to 2012 (11 years) were used in this study, which include (1) precipitation, (2) aerosol, (3) cloud, and (4) other meteorological fields.

#### 2.1.1 Precipitation data

To study diurnal variation of rainfall, the gauge-based hourly precipitation datasets were used, which were obtained from the National Meteorological Information Center (NMIC) of the China Meteorological Administration (CMA) (Yu et al., 2007) at 2420 stations in China from 1951 to 2012. The quality control made by CMA/NMIC includes the check for extreme values (the value exceeding the monthly maximum in daily precipitation was rejected), the internal consistency check (wiping off the erroneous records caused by incorrect units, reading, or coding) and spatial consistency check (comparing the time series of hourly precipitation with nearby stations) [Shen et al., 2010]. Here we chose 176 plain stations below the topography of 100 meter in BTH region, which is similar with our previous work because we purposely removed the orographic effect (Zhou et al., 2018). The record analyzed here is the period of 2002 to 2012.

**2.1.2 Aerosol data**

Aerosol optical depth (AOD), which is a proxy for the amount of aerosol particles in a column of the atmosphere and serves as an indicator for the division of the aerosol pollution condition in this study, was obtained from MODIS (Moderate Resolution Imaging Spectroradiometer) Collection 6 L3 aerosol product with the horizontal resolution of 1°x1° onboard the Terra satellite (Tao et al., 2015). The Collection 6 aerosol dataset is created from three separate retrieval algorithms that operate over different surface types: the two "Dark Target" (DT) algorithms for retrieving (1) over ocean (dark in visible and longer wavelengths) and (2) over vegetated/dark-soiled land (dark in the visible), plus the "Deep Blue" (DB) algorithm developed originally for retrieving (3) over desert/arid land (bright in the visible) (Levy et al., 2013). The merged data combing DB and DT retrievals in Collection 6 product was used in this study. The quality assurance of marginal or higher confidence was used in this study. The reported uncertainty in MODIS AOD data is on the order of (-0.02-10%), (+0.04+10%) (Levy et al., 2013). The Terra satellite overpass time at the equator is around 10:30 local solar time in the daytime, which we suppose is before the occurrence of most heavy rainfall events since the starting time of heavy rainfall is mostly after 12:00 LST (Fig. 1).

MACC-II (Monitoring Atmospheric Composition and Climate Interim Implementation) reanalysis product provided by ECMWF (the European Centre for Medium-Range Weather Forecasts), which assimilates total AOD retrieved by MODIS to correct for model departures from observed aerosols (Benedetti *et al*., 2009), provided the two-dimensional AOD and three-dimensional aerosol mass concentration datasets for different kinds of aerosols (BC, sulfate, organic matter, mineral dust and sea salt). MACC-II reanalysis products are observationally-based within a model framework, which can offer a more complete temporal and spatial coverage than observation and overcome the shortcoming of simulation that fail in simulating the complexity of real aerosol distributions. The horizontal resolution of MACC-II is 1°×1° and the vertical resolution is 60 levels. MACC-II data covers the period of 2003 to 2012, of which the time interval is six-hour.

**2.1.3 Cloud data**

Daily cloud variables, including cloud fraction (CF), cloud top pressure (CTP), cloud optical thickness (COT, liquid and ice), cloud water path (CWP, liquid and ice) and cloud effective radius (CER, liquid and ice), were obtained from MODIS Collection 6 L3 cloud product onboard the Terra satellite. The MODIS cloud product combines infrared emission and solar reflectance techniques to determine both physical and radiative cloud properties (Platnick et al., 2017). The validation of cloud top properties in this product has been conducted through comparisons with CALIOP (Cloud-Aerosol Lidar with Orthogonal Polarization) data and other lidar estimates using aircraft observations, and the validation and quality control of cloud optical products is performed primarily using in situ measurements obtained during field campaigns as well as the MODIS Airborne Simulator (MAS) instrument (https://modis-atmos.gsfc.nasa.gov/products/cloud). Likewise, the quality assurance of marginal or higher confidence was used in this study.

The three-dimensional cloud variables, such as CF, cloud liquid water and cloud ice water, were obtained from MERRA2 (the second Modern-Era Retrospective analysis for Research and Applications) reanalysis datasets. MERRA2 reanalysis data is undertaken by NASA for the satellite era using GEOS-5 (version 5 of the Goddard Earth Observing System Data Assimilation System), which is the first long-term global reanalysis to assimilate space-based observations of aerosols and represent their interactions with other physical processes in the climate system. The horizontal resolution is 0.624°x0.5° and the vertical resolution is 42 levels with three-hour intervals (Rienecker et al., 2008). Since the clouds associated with heavy rainfall in the BTH region during the early summer contain warm clouds, cold clouds and mixed-phase clouds (e.g. Guo et al., 2015), we purposely selected the clouds with its top pressure above 600 hPa because the 0°C isotherm of BTH region is nearly located at this height.

#### 2.1.4 Other meteorological data

Other meteorological factors, including the wind, temperature, and relative humidity (RH), were obtained from the ERA-Interim reanalysis datasets with 1°x1 °horizontal resolution and 37 vertical levels at six-hour intervals. ERA-Interim is the global atmospheric reanalysis produced by ECMWF, which covers the period from 1979 to near-real time (Dee et al., 2011). To unify the datasets, we interpolated the gridded datasets into stations using the average value in a 1°×1° grid as the background condition of each rainfall station.

## 2.2 Methodology

### 2.2.1 Selection of sub-season and circulation

Consistent with our previous work (Zhou et al., 2018), we focused on the early summer period (1 June to 20 July), which is before the start of the large-scale rainy season over the BTH region, to better identify the effect of aerosols on local convective precipitation. And to unify the background atmospheric circulation, we only selected the rainfall days with southwesterly flow, which is the dominant circulation (around 40%) over the BTH region during early summer (Zhou et al., 2018).

### 2.2.2 Classification of the heavy rainfall and clean/polluted conditions

With the circulation of southwesterly, we selected heavy rainfall samples when the hourly precipitation amount was more than 8.0 mm/hour (defined by *Atmospheric Sciences Thesaurus, 1994*). The 25$^{th}$ and 75$^{th}$ AOD (the value is 0.98 and 2.00 respectively) were used as the thresholds of clean and pollution condition. It shows that there are 514 cases of heavy rainfall on polluted days and 406 cases of that on clean days.

Using the same percentile method, we chose cases of more BC/sulfate when the AOD of BC/sulfate is larger than the 75$^{th}$ AOD of itself in all rainy days with southwesterly, and cases of less BC/sulfate when that is less than the 25$^{th}$ AOD of itself in the same condition. Accordingly, we selected 459 cases of more BC and 274 cases of less BC with heavy rainfall. Similarly, 361 cases of more sulfate and 419 cases of less sulfate with heavy rainfall were selected.

### 2.2.3 Statistical analysis

We adopted the probability distribution function (PDF) to compare the features of heavy rainfall and cloud variables on clean and pollution days or in different condition of aerosols, by which we can understand the changes of rainfall/cloud properties more comprehensively than by the mean state. Student's t-test was used to check the significance of all the differences of the variables between different conditions of pollution.

## 3 Distinct characteristics of heavy rainfall diurnal variation associated with aerosol pollution

Our previous study (Zhou et al. 2018) has reported the distinct peak shifts of rainfall diurnal variation between clean days and polluted days over the BTH region during early summer. The PDF of the heavy rainfall peak time shows that the peak time is about two hours earlier on the polluted days (20:00 LST) than that on the clean days (22:00 LST) (Fig. 1b). To comprehensively recognize the change of rainfall diurnal variation associated with air qualities, here we examined the PDF of the starting time, the duration and the intensity besides the peak time of heavy rainfall.

In terms of the starting time for the heavy rainfall, a significant advance of the starting time is found as shown in Fig. 1b. The time for maximum frequency of heavy rainfall initiation is 6 hours earlier on the polluted days, shifting from around 0:00 LST on the clean days to the 18:00 LST. Regarding the durations of heavy rainfall, the persistence of heavy rainfall on polluted days is nearly 0.8 hours longer than that on clean days. According to the PDF shown as in Fig. 1c, the occurrence of short-term precipitation (≤6 hours, Yuan et al., 2010) decreases while that of long-term precipitation (>6 hours, Yuan et al., 2010) increases. The intensity of hourly rainfall on the polluted days exhibits a decrease on the polluted days. However, compared with the other features, the change of intensity does not pass the 95% statistical confidence level. Therefore, the following only focuses on investigating why the starting time, peak time and duration of heavy rainfall change with pollution in diurnal time scale.

## 4 Cloud effect of aerosols with inclusion of moisture

### 4.1 Characteristics of clouds on clean and polluted days

To understand the cloud effect of aerosols on heavy rainfall diurnal variation, we need to recognize the associated cloud features on clean and polluted days. The differences of cloud diurnal features were examined in both macroscopic properties (including CF, CTP, COT and CWP) and microscopic properties (including CER) between the clean and polluted circumstances, as shown in Fig. 2. The PDF distribution of CF is significantly different between clean and polluted conditions, which shows that the CF with maximum occurrence frequency on the clean days is nearly 50% while reaches more than 90% on the polluted days. The PDF of CTP on the polluted days shows a decrease at 200-300 hPa but an increase at around 400 hPa with a mean increase of 24.3 hPa, which indicates the cloud top height is lower on the polluted days.

The COT, CWP and CER were further analyzed for the liquid and ice portions of clouds as shown in Fig. 2. Both liquid and ice COT on polluted days exhibit a significant increase compared with that on clean days. The mean amount of liquid COT increases by 3.9 and ice COT increases by 6.3. Similar with COT, the amount of liquid and ice CWP increase on polluted days. And the mean amount of liquid CWP increases by 40.3 $g/m^2$ and ice CWP increases by 94.4 $g/m^2$. The PDF of liquid CER also shows shifts to the larger size and its mean value increases by 0.6 μm on polluted days. In contrast with the CER of liquid clouds, the CER of ice clouds shows a slight shift to the smaller size with an averaged decrease of 2.8 μm. Thus, except for the ice CER, the other cloud variables consistently exhibit increases on the polluted days.

Figure 3 shows the distinct variation of three-dimensional cloud liquid/ice water on clean and polluted days as well as their differences. On clean days, the liquid clouds are mainly located between 300 hPa and 850 hPa, with two maximum layers respectively at 350 hPa and 700 hPa (Fig. 3a). The major characteristics are that the peak of liquid water occurs in the evening (at 20:00-23:00 LST) (Fig. 3a) while the ice water appears in the mid-night (at 20:00-3:00 LST) (Fig. 3d). Compared with clean condition, the amount of the liquid and ice water are both significantly increased on polluted days. Meanwhile, the peak value of liquid water appears much earlier by almost 8 hours than that on clean days. i.e., the peak of the liquid water occurs at 14:00 LST under pollution (Fig. 3b). The ice water exhibits the similar shift of its peak under pollution and its maximum center appears in the afternoon (at 14:00-17:00 LST) rather than the mid-night (Fig. 3e). The difference of ice water between polluted and clean condition also indicates that the cloud top on polluted days is lower than that on clean days (Fig. 3f), which is consistent with the result in Fig. 2.

According to the above results, the increased aerosols correspond to the increase of CF, COT, CWP of both liquid and ice clouds, and liquid CER but the decrease of cloud top height and ice CER. Additionally, the peaks of the liquid and ice water shift earlier on the polluted days.

### 4.2 Changes of cloud properties affected by moisture on clean and polluted days

The different moisture condition can influence the effect of aerosols on cloud properties (Yuan et al., 2008; Jiang et al., 2008; Jung et al., 2013; Qiu et al., 2017). It is hard to completely remove the moisture effect on the above results in a pure observational study, although we have fixed the wind direction in this study. Since the southwesterly circulation background cannot only transport pollutants but also moisture to the BTH region (Wu et al., 2017), more pollution usually corresponds to more moisture. And Figure 4a does show that the humidity increases accompanied with increased AOD over BTH region. Because the moisture supply for BTH is mainly transported via low-level southwesterly circulation, we purposely use the RH at 850 hPa as the indicator of moisture condition. The PDF of humidity shows that the 40-60% RH dominates the clean cases while 60-90% RH dominates the polluted cases (Fig. 4b), which indicates that the above changes of cloud properties on the polluted days in Sect. 4.1 often occur in the condition of higher RH. To identify the effect of aerosols on the properties of clouds, we purposely investigated the changes of cloud properties with inclusion of moisture change respectively on the clean days and polluted days (Fig. 5).

A common feature is that all examined variables of clouds exhibit increases along with the increase of moisture on both clean and polluted days (Fig. 5). If fixing the moisture, the amounts of CF, COT (both liquid and ice), CWP (both liquid and ice) become larger on the polluted days, which are consistent with the above-mentioned results without removing the moisture effect in Sect. 4.1. However, the aerosol effect on CTP is evidently distinct between low and high RH conditions (Fig. 5f). When the RH is relatively low (<70%), the amount of CTP on polluted days is larger than that on clean days. In contrast, the CTP becomes smaller when the RH is relatively high (>70%). That is to say, aerosols reduce the cloud top at lower RH but increase it at higher RH.

As Fig. 4b has shown, usually the RH is lower (40-60%) on clean days and higher (60-90%) on polluted days. The average of CTP on clean days at the RH of 40-60% is nearly 350 hPa but 420 hPa on polluted days with the RH of 60-90% (Fig. 5d). Therefore, the cloud top on polluted days is normally lower than that in clean cases, which is consistent with the result in Sect. 4.1. In summary, although the aerosols can lift the cloud top when RH is higher, the cloud top on polluted days is still lower than that on clean days due to their different moisture conditions.

To examine if the aerosol effect on cloud microphysical property is modified by moisture, we further investigated the variation of the CER between clean and polluted condition along with different CWPs, as shown in Fig. 6. The result exhibits that aerosol effect on liquid CER is modified by CWP. When the CWP is smaller than 60 $g/m^2$, increased aerosols reduce CER; When the CWP is larger than 60 $g/m^2$, CER on polluted days becomes larger. Different from the situation of liquid CER, ice CER on polluted days is always smaller than that on clean days when fixing the ice CWP (Fig. 6).

### 4.3 Possible effect of aerosols on cloud with inclusion of moisture

We attempt to understand the above results of aerosol effect on clouds with inclusion of moisture. The aerosols serving as CCN nucleate a larger number of cloud droplets and accumulate more liquid water in the cloud, so the CF, COT and CWP become increased. However, why the aerosol effect on cloud top and liquid CER depends on different moisture conditions has not been clarified yet.

In terms of cloud top, we speculate the following mechanisms in clean and polluted condition. On the clean days with fewer moisture, the fewer cloud droplets cause the delayed precipitation due to relatively depressed collision-coalescence process, thus the clouds tend to develop vertically to a higher altitude, which also corresponds to the delayed formation of ice clouds (Fig. 3d). On the polluted days, the increased aerosols (CCN) can increase the cloud droplet number (Squires and Twomey, 1966), which can enhance the collision-coalescence process (Rosenfeld, 1999; Liu et al., 2003). When the moisture supply is sufficient, the cloud drops can become larger via adequate collision-coalescence and easily convert to rain drops, which facilitates the advance of rainfall start. After the rainfall started, the cloud top is restricted to grow higher. Therefore, the cloud top exhibits relatively lower in polluted cases over BTH region (Fig. 3f).

For liquid CER, when moisture supply is fixed, aerosols serve as CCN nucleating larger number concentrations of cloud drops but smaller size of droplets, which is Towmey effect (Albrecht 1989; Rosenfeld et al. 2014). However, because the heavy pollution in BTH region is usually accompanied with high humidity supply (Fig. 4), the aerosol effect on cloud exhibits "anti-Towmey" effect (Yuan et al., 2008; Jung et al., 2013; Qiu et al., 2017). i.e., the aerosols increase both the number and the size of cloud droplet via enhanced collision-coalescence due to the plenty of moisture supply.

However, the above mechanisms cannot work for the ice CER. The study has shown the ice CWP increases but the ice CER decreases under pollution. We assume the aerosols increase the cloud droplets so that reduce the vapor pressure inside clouds, thus decrease the supersaturation and weaken the process of transitions from liquid droplet into ice crystal, which is known as Bergeron process (Squires, 1952). So far the detailed physical processes of cold clouds and mixed-phase clouds are not clear, including the diffusional grow, accretion, riming and melting process of ice precipitation (Cheng et al., 2010), which needs numerical model simulations to further explore.

## 5 Aerosol radiative effect and cloud effect on rainfall diurnal variation

Our previous study has indicated that the radiative effect of BC low-level warming may facilitate the convective rainfall generation (Zhou et al., 2018). Based on the changes of cloud properties addressed in Sect. 4, we further attempt to understand the different roles of aerosol radiative heating effect and cloud effect on modifying the diurnal variation of heavy rainfall through the two aerosol types-BC and sulfate, which both have their maximum centers over BTH in China (Fig. 7). The sulfate is one of the most effective CCN that influences the cloud and precipitation in the BTH region (Gunthe et al., 2011). We purposely selected the cases with different BC/sulfate concentrations to compare the role of BC/sulfate on the diurnal variation of the heavy rainfall. The methods have been described in Sect. 2.2.2.

The PDF of the starting time, peak time and duration of heavy rainfall were examined for the higher and lower BC concentrations (Fig. 8a), respectively. The most striking result is that the starting time of heavy rainfall in high BC concentrations evidently shifts earlier by 7 hours from 19:00 LST to 2:00 LST. Meanwhile, compared with low BC cases, the peak time of heavy rainfall in high BC cases is more distinguishable and shows an increase in the evening but a decrease at midnight to early morning. And the duration time of heavy rainfall is slightly shorter in high BC cases. In contrast, when the sulfate has higher concentrations, the starting time of heavy rainfall is evidently delayed while the duration time of heavy rainfall shows a significant increase. The peak time of heavy rainfall occurrence also shows earlier and mainly locates at around 21:00 LST but not as significant as that for high BC cases (Fig. 8b).

We also compared the effect of BC/sulfate on the associated cloud to identify the cloud effect of the two types of aerosols. We found more BC corresponds to a slight decrease of CF when CF is more than 90% (Fig. 9), which might be associated with semi-direct effect of BC (IPCC, 2013). By comparison, the CF increases significantly with increased sulfate concentrations when CF is above 90%. The sharp increase of CF with increased sulfate indicates that the CF is very sensitive to sulfate-like aerosols. Accordingly, the changes of other cloud variables under pollution as above mentioned are also likely associated with this type of aerosols, which can serve as CCN and influence the cloud properties.

The earlier start of heavy rainfall and the decrease of CF in high BC cases denote that BC influences the heavy rainfall through changing the thermodynamic condition of atmosphere (Zhou et al., 2018), which increases upward motion and accelerates the formation of cloud and rainfall. Thus, BC heating effect should play a dominant role in the beginning of rainfall. The delayed start and advanced peak of heavy rainfall with higher sulfate concentrations indicate that the increased sulfate may accelerate the rainfall process from the initial to the peak stage through enhancing the collision-coalescence and improving the efficiency of precipitation in the condition of sufficient moisture. The longer duration in high sulfate cases corresponds to that the sulfate as CCN increases the amount of cloud and lengthens the rainfall duration because of sufficient moisture supply. Therefore, when the BTH pollution is relatively heavy, the moisture supply is usually sufficient. In this situation, increased BC concentrations advance the beginning time and sharpen the peak time via the radiative effect, while more sulfate aerosols accelerate the rainfall to the peak and remarkably extend the duration time of heavy rainfall through the cloud effect.

## 6. Conclusions

Using the gauge-based hourly rainfall records, aerosol and cloud satellite products and high temporal resolution reanalysis datasets during 2002-2012, this study found the starting and peak time of heavy rainfall occur earlier and the rainfall duration becomes longer under pollution. By comparing the characteristics of cloud macrophysics and microphysics variables, we found the CF, COT (liquid and ice), CWP (liquid and ice) and liquid CER are increased in polluted condition, but the cloud top height and the ice CER are reduced under pollution. We also investigated if the moisture influences the aerosol cloud effect, and found that the aerosol effect on CF, COT (liquid and ice), CWP (liquid and ice) and ice CER does not depend on the moisture condition. However, the aerosol effect on the cloud top height and liquid CER are opposite between at lower and higher moisture conditions. The different roles of BC and sulfate on modifying the diurnal shift were also examined. We found that higher BC concentrations correspond to the earlier start and peak of heavy rainfall while higher sulfate concentrations correspond to earlier peak and longer duration of heavy rainfall. The two different types of aerosols play different roles on different stages of rainfall development.

As a summary using a schematic diagram (Figure 10) to illustrate how aerosols modify the diurnal variation of heavy rainfall over BTH region. On one hand, BC absorbs shortwave radiation during the daytime and warms the lower troposphere, and then increases the instability of the lower to middle atmosphere so that enhances the local upward motion and moisture convergence. As a result, the BC-induced thermodynamic instability of the atmosphere triggers the occurrence of heavy rainfall in advance (Zhou et al. 2018). On the other hand, the increased upward motion transports more sulfate-like particles into the clouds so that more CCN and sufficient moisture increase the cloud droplet number and cloud water, thus enhancing the collision-coalescence and accelerating the conversion of cloud droplets into rain droplets (Johnson, 1982; Cheng et al., 2007), which enhances the efficiency of rainfall and advances the arrival of rainfall peak. Additionally, the increased CCN nucleates more cloud droplets and accumulates more liquid water in clouds, the duration of heavy rainfall is accordingly prolonged.

Although this work has attempted to exclude the impacts from the meteorological background particularly circulation and moisture, the observation study still has its limitation on studying aerosol effect on rainfall, such as the noise and uncertainty of different observational data, the interaction of aerosol and meteorological factors and the mixing of different types of aerosols. Numerical model simulations are needed to examine the mechanism we proposed here. And the process of aerosols effect on the ice cloud precipitation formation also needs further exploration in our future study.

**Data availability**

We are grateful to the National Meteorological Information Centre (NMIC) of the China Meteorological Administration (CMA) for providing hourly precipitation datasets. MODIS aerosol and cloud data were obtained from http://ladsweb.modaps.eosdis.nasa.gov; MERRA2 reanalysis data were obtained from https://disc.gsfc.nasa.gov/daac-bin/FTPSubset2.pl; MACC-II and ERA-interim reanalysis datasets were obtained from http://apps.ecmwf.int/datasets.

**Author contributions**

JY conceived the study. SZ processed data and drew the figures. SZ and JY analyzed the observational results and CZ, WCW, and DG gave the professional guidance. PS provided the hourly precipitation dataset. SZ and JY prepared the manuscript with contributions from CZ and WCW.

**Competing interests**

The authors declare that they have no conflict of interest.

**Acknowledgements**

This study is supported by funds from the National Key Research and Development Program-Global Change and Mitigation Project: Global Change Risk of Population and Economic System: Mechanism and Assessment (2016YFA0602401), the National Natural Science Foundation of China (grant nos. 41375003, 41621061 and 41575143) and Project supported by State Key Laboratory of Earth Surface Processes and Resource Ecology and Key Laboratory of Environmental Change and Natural Disaster. Wei-Chyung Wang acknowledges the support of a grant (to SUNYA) from the Office of Sciences (BER), U.S. DOE.

**References:**

Albrecht, B. A.: Aerosols, cloud microphysics, and fractional cloudiness, Science 245: 1227-1230, 1989.

Anonymous: 1994. Atmospheric Sciences Thesaurus. China Meteorological Press: Beijing, China. (in Chinese)

Anonymous (2013), IPCC fifth assessment report,Weather, 68, 310-310.

Bellouin, N., Quaas, J., Morcrette J. -J., and Boucher, O.: Estimates of aerosol radiative forcing from the MACC re-analysis. Atmos. Chem. Phys., 13: 2045-2062, 2013.

Benedetti, A., Morcrette, J. J., Boucher, O., Dethof, A., Engelen, R. J., Fisher, M., Flentje, H., Huneeus, N., Jones, L., Kaiser, J. W., Kinne, S., Mangold, A., Razinger, M., Simmons, A. J., and Suttie, M.: Aerosol analysis and forecast in the European Centre for Medium-Range Weather Forecasts Integrated Forecast System: 2. Data assimilation. J. Geophys. Res. 114: D13205 doi:10.1029/2008JD011115, 2009.

Bulgin, C. E., Palmer, P. I., Thomas, G. E., Arnold, C. P. G., Campmany, E., Carboni, E., Grainger, R. G., Poulsen, C., Siddans, R., and Lawrence, B. N.: Regional and seasonal variations of the Twomey indirect effect as observed by the ATSR-2 satellite instrument, Geophys. Res. Lett. 35, L02811, doi:10.1029/2007GL031394, 2008.

Chen, Q., Yin, Y., Jin, L., Xiao, H., and Zhu, S.: The effect of aerosol layers on convective cloud microphysics and precipitation, Atmos. Res., **101,** 327-340, 2011.

Cheng, C. T., Wang, W. C., and Chen, J. P.: A modeling study of aerosol impacts on cloud microphysics and radiative properties, Q. J. R. Meteorol. Soc., 133, 283–297, doi:10.1002/qj.25, 2007.

Cheng, C. T., Wang, W. C., and Chen, J. P.: Simulation of the effects of increasing cloud condensation nuclei on mixed-phase clouds and precipitation of a front system. Atmos. Res., 96: 461-476, doi: 10.1016/j.atmosres.2010.02.005, 2010.

A modeling study of aerosol impacts on cloud microphysics and radiative properties, Q. J. R. Meteorol. Soc., 133, 283–297, doi:10.1002/qj.25, 2010.

Dee, D. P., Uppala, S. M., Simmons, A. J., Berrisford, P., Poli, P., Kobayashi, S., Andrae, U., Balmaseda, M. A., Balsamo, G., Bauer, P., Bechtold, P., Beljaars, A. C. M., van de Berg, L,, Bidlot, J., Bormann, N., Delsol, C., Dragani, R., Fuentes, M., Geer, A. J., Haimberger, L., Healy, S. B., Hersbach, H., H´olm, E. V., Isaksen, L., K°allberg, P., K¨ohler, M., Matricardi, M., McNally, A. P., Monge-Sanz, B. M., Morcrette, J. –J., Park, B. –K., Peubey, C., de Rosnay, P., Tavolato, C., Th´epaut, J. –N., Vitart, F.: The ERA-Interim reanalysis: configuration and performance of the data assimilation system. Q. J. R. Meteorol. Soc. 137: 553–597. DOI:10.1002/qj.828, 2011.

Fan, J. W., Rosenfeld, D., Yang, Y., Zhao, C., Leung, L. R., and Li, Z. Q.: Substantial contribution of anthropogenic air pollution to catastrophic floods in Southwest China. Geophys. Res. Lett. 42: 6066-6075, 2015.

Garrett, T. J. and Zhao, C.: Increased Arctic cloud longwave emissivity associated with pollution from mid-latitudes. Nature 440(7085): 787-9, 2006.

Givati, A., and Rosenfeld, D.: Quantifying precipitation suppression due to air pollution. J. Appl. Meteor. 43: 1038-1056, 2004.

Gunthe, S. S., Rose, D., Su, H., Garland, R. M., Achtert, P., Nowak, A., Wiedensohler, A., Kuwata, M., Takegawa, N., Kondo, Y., Hu, M., Shao, M., Zhu, T., Andreae, M. O., and Poschl, U.: Cloud condensation nuclei (CCN) from fresh and aged air pollution in the megacity region of Beijing, Atmos. Chem. Phys. 11(21): 11023-11039, 2011.

Guo, C. W., Xiao, H., Yang, H. L., and Tang, Q.: Observation and modeling analyses of the macro-and microphysical characteristics of a heavy rain storm in Beijing, Atmos. Res., 156: 125-141, DOI: 10.1016/j.atmosres.2015.01.007, 2015.

Guo, J. P., Deng, M. J., Lee, S. S., Wang, F., Li, Z. Q., Zhai, P. M., Liu, H., Lv, W., Yao, W., and Li, X. W.: Delaying precipitation and lightning by air pollution over the Pearl River Delta. Part I: Observational analyses. J. Geophys. Res. Atmos. 121: 6472-6488, 2016.

Guo, L., Highwood, E. J., Shaffrey, L. C., and Turner, A. G.: The effect of regional changes in anthropogenic aerosols on rainfall of the East Asian Summer Monsoon. Atmos. Chem. Phys. 13: 1521-1534, 2013.

Guo, X. L., Fu, D. H., Guo, X., and Zhang, C. M.: A case study of aerosol impacts on summer convective clouds and precipitation over northern China. Atmos. Res.142: 142-157, 2014.

Harikishan, G., Padmakumari, B., Maheskumar, R. S., Pandithurai, G., and Min, Q. L.: Aerosol indirect effects from ground-based retrievals over the rain shadow region in Indian subcontinent, J. Geophys. Res. Atmos.

121(5): 2369-2382, 2016.

Jacobson, M. Z.: Strong radiative heating due to the mixing state of black carbon in atmospheric aerosols. Nature 409: 695-697, 2001.

Jiang, H., Feingold, G., and Cotton, W. R.: Simulations of aerosol-cloud-dynamical feedbacks resulting from entrainment of aerosol into the marine boundary layer during the Atlantic Stratocumulus Transition Experiment, J. Geophys. Res., 107(D24), 4813, doi:10.1029/2001JD001502, 2002.

Jiang, J. H., Su, H., Schoeberl, M. R., Massie, S. T., Colarco, P., Platnick, S., and Livesey, N. J.: Clean and polluted clouds: Relationships among pollution, ice clouds, and precipitation in South America, Geophys. Res. Lett., 35, L14804, doi: 10.1029/2008GL034631, 2008.

Jiang, M. J., Li, Z. Q., Wan, B. C., and Cribb, M.: Impact of aerosols on precipitation from deep convective clouds in eastern China. J. Geophys. Res. 121: 9607-9620, 2016.

Johnson, D. B.: The role of giant and ultra-giant aerosol particles in warm rain initiation, J. Atmos. Sci., 39, 448–460, doi:10.1175/1520-0469(1982)039<0448:TROGAU>2.0.CO;2, 1982.

Jung, W. S., Panicker, A. S., Lee, D. I., and Park, S. H.: Estimates of aerosol indirect effect from Terra MODIS over Republic of Korea, Advances in Meteorology, 2013 (976813): 1-8, http://dx.doi.org/10.1155/2013/976813, 2013.

Lau, K. M., Kim, M. K., and Kim, K. M.: Asian summer monsoon anomalies induced by aerosol direct forcing: the role of the Tibetan Plateau. Clim. Dyn., 26: 855-864, 2006.

Lee, S. S., Donner, L. J., and Phillips, V. T. J.: Impacts of aerosol chemical composition on microphysics and precipitation in deep convection. Atmos. Res., 94, 220-237, 2009.

Lee, S. S., Guo, J., and Li, Z: Delaying precipitation by air pollution over the Pearl River Delta: 2. Model simulation. J. Geophys. Res. Atmos., 121: 11739-11760, 2016.

Lelieveld, J. and Heintzenberg, J.: Sulfate cooling effect on climate through in-cloud oxidation of anthropogenic SO2. Science 258: 117-120, 1992.

Levy, R. C., Mattoo, S., Munchak, L. A., Remer, L. A., Sayer, A. M., Patadia, F., and Hsu, N. C.: The Collection 6 MODIS aerosol products over land and ocean, Atmos. Meas. Tech., 6, 2989–3034, https://doi.org/10.5194/amt-6-2989-2013, 2013.

Li, Z., Niu, F., Fan, J., Liu, Y., Rosenfeld, D., and Ding, Y.: Long-term impacts of aerosols on the vertical development of clouds and precipitation, Nat. Geosci., 4, 888-894, 2011.

Lim, K. S. and Hong, S.: Investigation of aerosol indirect effects on simulated flash-flood heavy rainfall over Korea, Meteor. Atmos. Phys., **118,** 199-214, 2012.

Liu, G., Shao, H., Coakley Jr. J. A., Curry, J. A., Haggerty, J. A., and Tschudi, M. A.: Retrieval of cloud droplet size from visible and microwave radiometric measurements during INDOEX: Implication to aerosols' indirect radioactive effect, J. Geophys. Res., 108(D1), 4006, doi:10.1029/2001JD001395, 2003.

Panicker, A. S., Pandithurai, G., and Dipu, S.: Aerosol indirect effect during successive contrasting monsoon seasons over Indian subcontinent using MODIS data, Atmospheric environment 44(15): 1937-1943,

Atmos. Chem. Phys. Discuss., https://doi.org/10.5194/acp-2018-1072
Manuscript under review for journal Atmos. Chem. Phys.
Discussion started: 16 November 2018



2010.

Platnick, S., Meyer, K., King, M. D., Wind, G., Amarasinghe, N., Marchant, B., Arnold, G. T., Zhang, Z., Hubanks, P. A., Holz, R. E., Yang, P., Ridgway, W. L., and Riedi, J.: The MODIS cloud optical and microphysical products: Collection 6 updates and examples from Terra and Aqua. IEEE Trans. Geosci. Remote Sens., 55, 502-525, doi:10.1109/TGRS.2016.2610522, 2017

Qiu, Y., Zhao, C., Guo, J., and Li, J.: 8-Year ground-based observational analysis about the seasonal variation of the aerosol-cloud droplet effective radius relationship at SGP site. Atmos. Environ. 164: 139-146, 2017.

Rienecker, M. M., Suarez, M. J., Todling, R., Bacmeister, J., Takacs, L., Liu, H. C., Gu, W., Sienkiewicz, M., Koster, R. D., Gelaro, R., Stajner, I., Nielsen, J. E.: The GEOS-5 Data Assimilation System—Documentation of Versions 5.0.1 and 5.1.0, and 5.2.0. NASA Technical Report Series on Global Modeling and Data Assimilation NASA/TM-2008 -104606 27: 92 pp, 2008.

Rosenfeld, D.: TRMM observed first direct evidence of smoke from forest fires inhibiting rainfall, Geophys. Res. Lett., 26, 3105–3108, doi:10.1029/1999GL006066, 1999.

Rosenfeld, D., Lohmann, U., Raga, G. B., O'Dowd, C. D., Kulmala, M., Fuzzi, S., Reissell, A., Andreae, M. O.: Flood or drought: How do aerosols affect precipitation?. Science 321:1309-1313, 2008.

Rosenfeld, D., Sherwood, S., Wood, R., and Donner, L.: Climate effects of aerosol-cloud interactions. Science 343: 379-380, 2014.

Rosenfeld, D., and Woodley, W. L.: Convective clouds with sustained highly supercooled liquid water down to _37_C, Nature, 405, 440–442, doi:10.1038/35013030, 2000.

Sassen, K., Starr, D., Mace, G. G., Poellot, M. R., Melfi, S. H., Eberhard, W.L., Spinhirne, J. D., Eloranta, E. W., Hagan, D. E., and Hallett, J.: The 5–6 December 1991 FIRE IFO II jet stream cirrus case study: Possible influences of volcanic aerosols, J. Atmos. Sci., 52, 97–123, doi:10.1175/1520-0469(1995) 052<0097:TDFIIJ>2.0.CO;2, 1995.

Shen, Y., Xiong, A., Wang, Y., and Xie, P.: Performance of high-resolution satellite precipitation products over China, J. Geophys. Res., 115, D02114, doi:10.1029/2009JD012097, 2010.

Sherwood, S.: Aerosols and ice particle size in tropical cumulonimbus, J. Clim., 15, 1051–1063, doi:10.1175/1520-0442(2002)015<1051:AAIPSI>2.0.CO;2, 2002.

Song, X. L. and Zhang, G. J.: Microphysics parameterization for connective clouds in a global climate model: Description and single-column model tests, J. Geophys. Res. Atmos., 116, D02201, 2011.

Squires, P.: The growth of cloud drops by condensation: I. general characteristics, Aust. J. Sci. Res., Ser. A, 5, 66–86, 1952.

Squires, P., and Twomey, S.: A comparison of cloud nucleus measurements over central North America and Caribbean Sea, J. Atmos. Sci., 23, 401–404, doi: 10.1175/1520-0469(1966)023<0401:ACOCNM>2.0.CO;2, 1966.

Tao, M. H., Chen, L. F., Wang, Z. F., Tao, J. H., Che, H. Z., Wang, X. H., and Wang, Y.: Comparison and evaluation of the MODIS Collection 6 aerosol data in China. J. Geophys. Res. Atmos. 120:6992-7005, 2015.

Tao, W. K., Chen, J. P., Li, Z., Wang, C., and Zhang C.: Impact of aerosols on convective clouds and precipitation. Rev. Geophy., 50, RG2001/2012: 1-62, DOI: 10.1029/2011RG000369, 2012.

Twomey, S.: The influence of pollution on the shortwave albedo of clouds, J. Atmos. Sci., 34, 1149–1152, doi:10.1175/1520-0469(1977)034<1149:TIOPOT>2.0.CO;2, 1977.

Wang, J., Feng, J., Wu, Q., and Z. Yan, Z.: Impact of anthropogenic aerosols on summer precipitation in the Beijing-Tianjin-Hebei urban agglomeration in China: Regional climate modeling using WRF-Chem. Adv. Atmos. Sci., **33,** 753-766, 2016.

Wang, Z., Guo, P., and Zhang, H.: A Numerical Study of Direct Radiative Forcing Due to Black Carbon and Its Effects on the Summer Precipitation in China. Climatic and Environmental Research, **14,** 161-171, 2009.

Wu, P., Ding, Y. H., and Liu, Y. J.: Atmospheric circulation and dynamic mechanism for persistent haze events in the Beijing-Tianjin-Hebei region, Adv. Atmos. Sci.,34(4): 429-440, 2017.

Yang, X., Zhao, C., Zhou, L., Li, Z., Cribb, M., and Yang, S.: Wintertime cooling and a potential connection with transported aerosols in Hong Kong during recent decades. Atmos. Res. 211: 52-61, 2018.

Yu, R. C., Zhou, T. J., Xiong, A. Y., Zhu, Y. J., and Li, J. M.: Diurnal variations of summer precipitation over contiguous China. Geophys. Res. Lett. 34: L017041, 2007.

Yuan, T., Li, Z., Zhang, R., and Fan, J.: Increase of cloud droplet size with aerosol optical depth: An observation and modeling study. J. Geophys. Res. Atmos., 113: D04201, 2008.

Yuan, W. H., Yu, R. C., Chen, H. M., Li, J., and Zhang, M. H.: Subseasonal Characteristics of Diurnal Variation in Summer Monsoon Rainfall over Central Eastern China. J. Climate 23:6684-6695, 2010.

Zhou, S., Yang, J., Wang, W. C., Gong, D., Shi, P., and Gao, M.: Shift of daily rainfall peaks over the Beijing– Tianjin– Hebei region: An indication of pollutant effects? Int. J. Climatol. 2018:1–10. https://doi.org/10.1002/joc.5700, 2018.

**Figure captions**

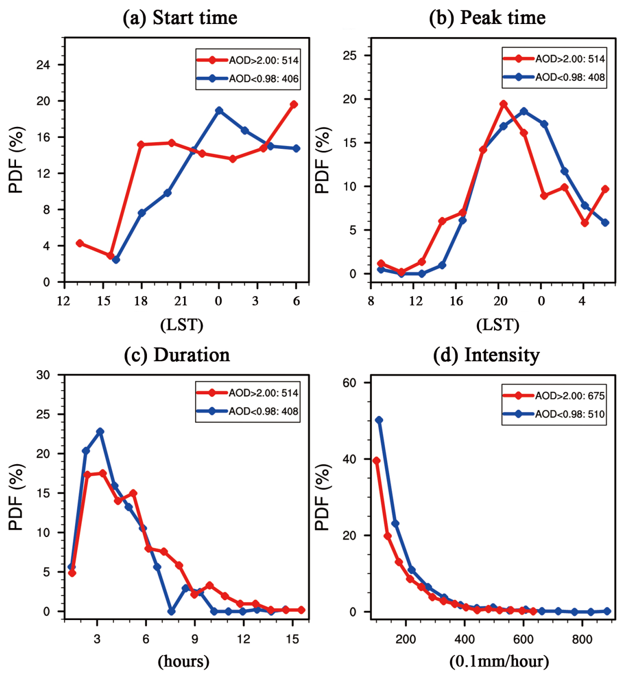


Figure 1. PDF of (a) starting time (units: LST), (b) peak time (units: LST), (c) duration (units: hours) and (d) intensity (units: 0.1mm/hour) of heavy rainfall on selected clean (blue lines: AOD<0.98) and polluted (red lines: AOD>2.00) days, respectively, during early summers from 2002 to 2012.

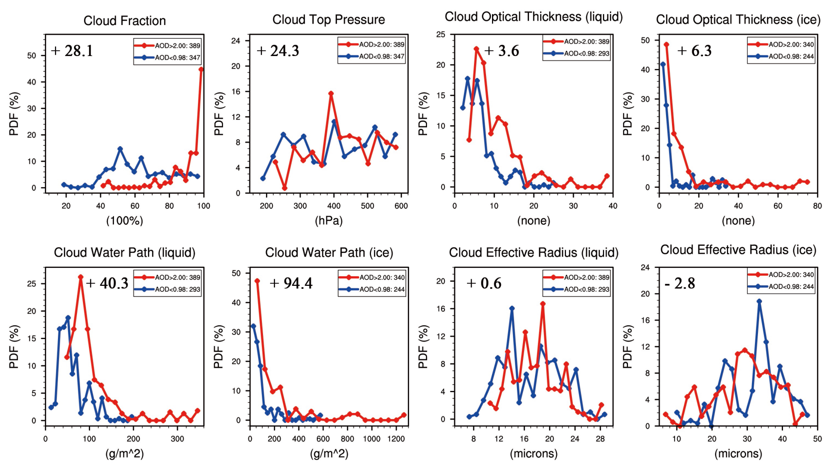


Figure 2. PDF of CF(units: %), CTP (units: hPa), COT (liquid and ice, units: none), CWP (liquid and ice, units:

Atmos. Chem. Phys. Discuss., https://doi.org/10.5194/acp-2018-1072
Manuscript under review for journal Atmos. Chem. Phys.
Discussion started: 16 November 2018


Atmospheric Chemistry and Physics
Open Access
Discussions

g/m$^2$) and CER (liquid and ice, units: microns) on selected clean (blue lines: AOD<0.98) and polluted (red lines: AOD>2.00) heavy rainfall days. The numbers in the upper left stand for the mean differences between polluted and clean days (polluted minus clean). Here we removed the cases with the cloud top pressure more than 600hPa during 11 early summers (2002-2012). The differences between clean and polluted cases have all passed the significant test of 95%.

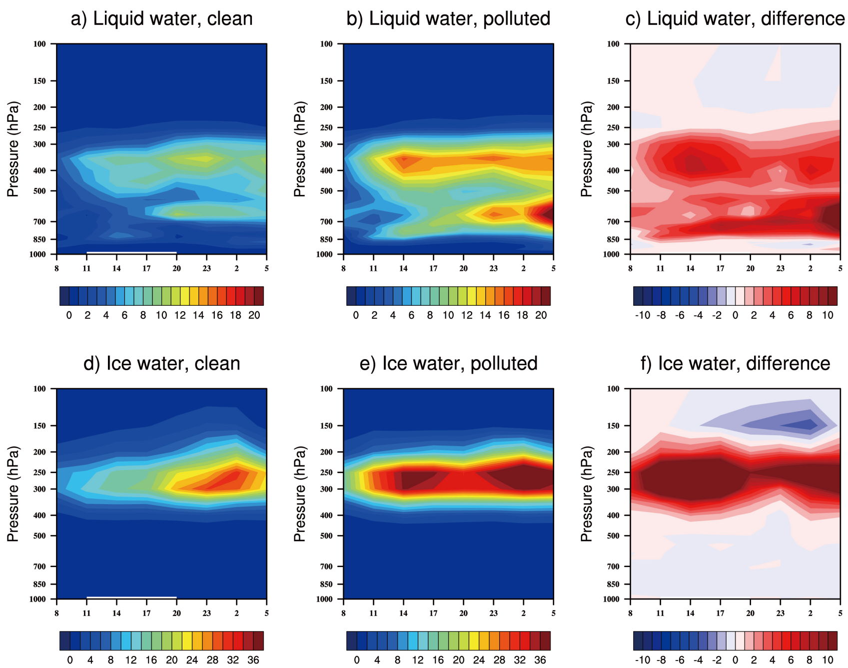


Figure 3. Diurnal variation of cloud liquid water (units: mg/kg) respectively for (a) clean days, (b) polluted days and (c) difference (polluted minus clean), and cloud ice water (units: mg/kg) respectively for (d) clean days, (e) polluted days and (f) difference (polluted minus clean). Differences have passed 95% significant test.

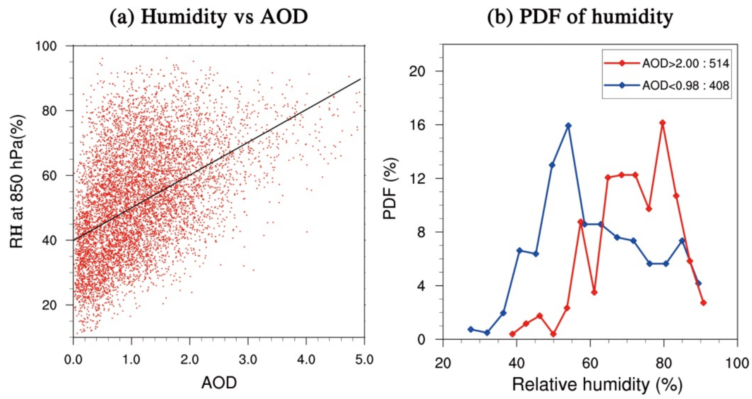


Figure 4. (a) Scatter plots of 850 hPa RH along with AOD variation (dotted) and the black line denotes the linear regression between AOD and RH. (b) PDF of 850 hPa RH respectively on clean (blue lines: AOD<0.98) and polluted (red lines: AOD>2.00) heavy rainfall days in the background of southwesterly.

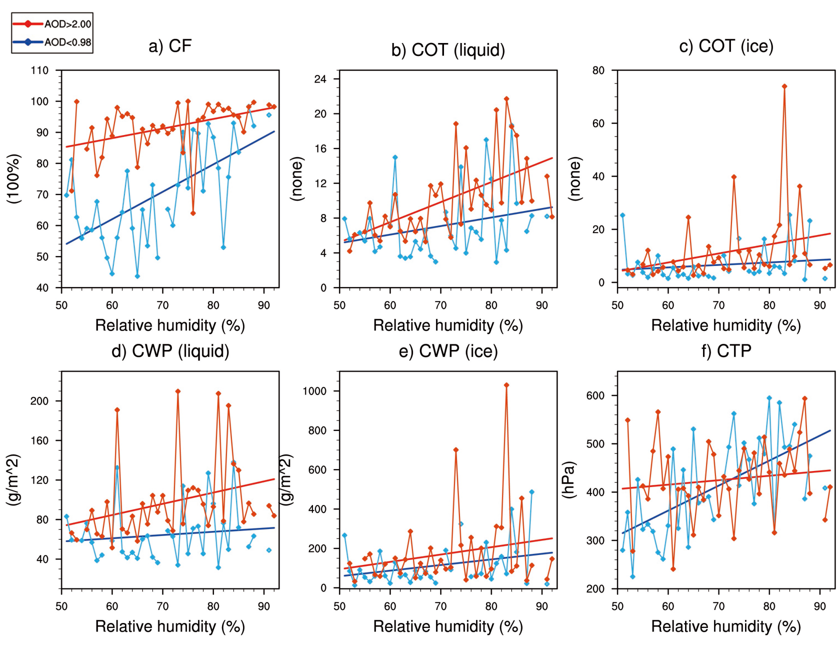


Figure 5. The changes of CF (units: %), COT (liquid and ice, units: none), CWP (liquid and ice, units: g/m$^2$) and CTP (units: hPa) along with the variation of the 850 hPa RH on selected clean (blue lines: AOD<0.98) and polluted (red lines: AOD>2.00) heavy rainfall days during 11 summers (2002-2012). The blue and red straight lines show the linear regressions. The trends have all passed the significant test of 95%.

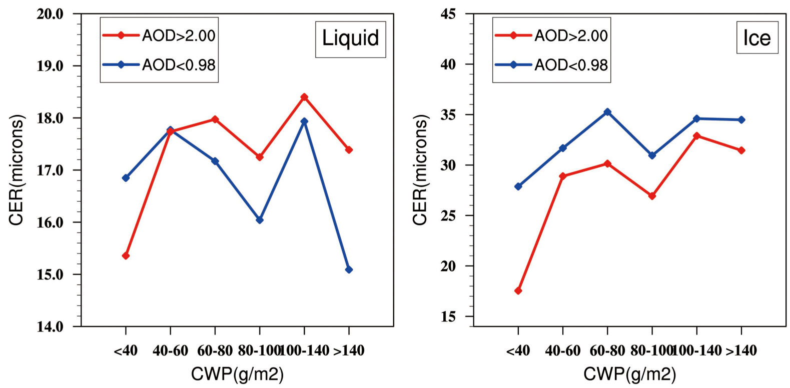


Figure 6. CER (units: microns) in different conditions of CWP (units: g/m$^2$) on clean (blue lines: AOD<0.98) and polluted (red lines: AOD>2.00) days respectively for liquid and ice clouds.

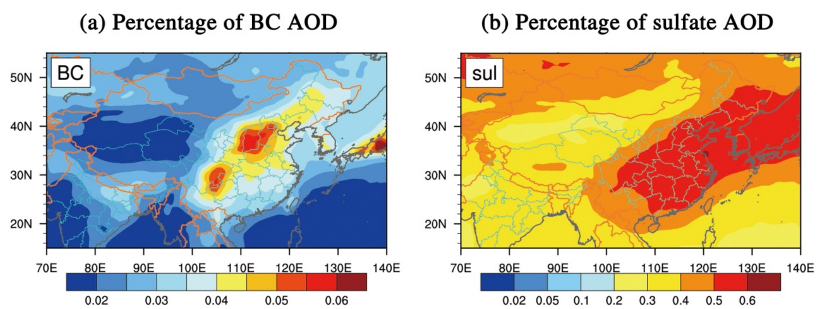


Figure 7. Percentages of AOD for (a) BC and (b) sulfate in JJA during 2002 to 2012.

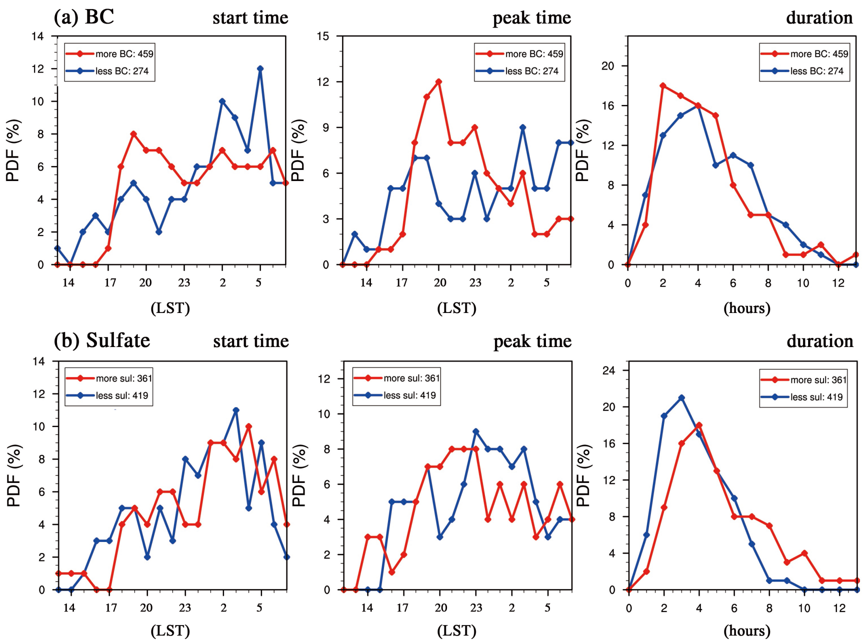


Figure 8. PDF of starting time (units: LST), peak time (units: LST) and duration (units: hours) of heavy rainfall in different conditions of (a) BC and (b) sulfate. Blue/red lines stand for the condition of less/more BC or sulfate during early summers from 2003 to 2012. The results have passed the significant test of 95%.

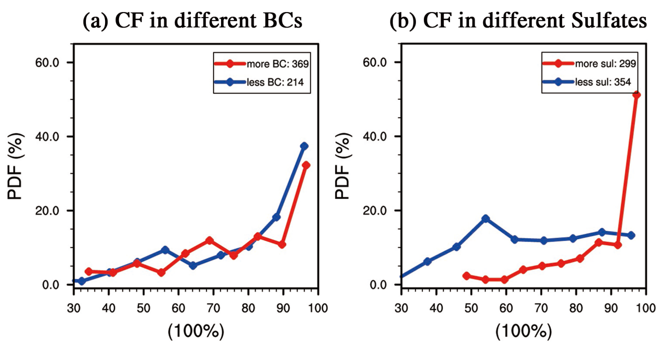


Figure 9. PDF of CF (units: 100%) respectively for selected less BC/sulfate (blue lines) and more BC/sulfate (red lines) cases with heavy rainfall and the cloud top pressure less than 600hPa during 10 early summers (2003-2012).

Atmos. Chem. Phys. Discuss., https://doi.org/10.5194/acp-2018-1072
Manuscript under review for journal Atmos. Chem. Phys.
Discussion started: 16 November 2018


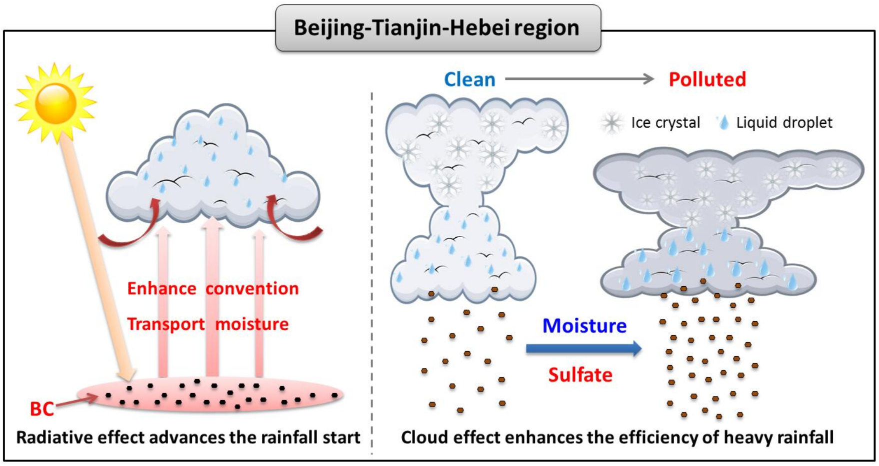


609

610 Figure 10. A schematic diagram for aerosols impact on the diurnal variation of heavy rainfall over
611 Beijing-Tianjin-Hebei region.

612

613

614